Rapid Communications | Editors' Suggestion

Hund's metal physics: From $SrNiO_2$ to $LaNiO_2$

Y. Wang [1], C.-J. Kang [2], H. Miao,[3] and G. Kotliar[1,2]

[1]*Department of Condensed Matter Physics and Materials Science, Brookhaven National Laboratory, Upton, New York 11973, USA*

[2]*Department of Physics and Astronomy, Rutgers University, Piscataway, New Jersey 08856, USA*

[3]*Material Science and Technology Division, Oak Ridge National Laboratory, Oak Ridge, Tennessee 37830, USA*

(Received 27 June 2020; revised 9 September 2020; accepted 15 October 2020; published 29 October 2020)

We study the normal state electronic structure of the recently discovered infinite-layer nickelate superconductor, $Nd_{1-x}Sr_xNiO_2$, using density functional theory plus dynamical mean-field theory calculations. Starting with the multiorbital compound $SrNiO_2$, our calculations show that despite large charge-carrier doping from $SrNiO_2$ to $LaNiO_2$, the Ni-3d total occupancy is barely changed due to the decreased hybridization with the occupied oxygen-2p states and increased hybridization with the unoccupied La-5d states. Thus, using $SrNiO_2$ as a reference, $La_{1-x}Sr_xNiO_2$ is naturally and conclusively found to be a multiorbital electronic system with characteristic Hund's metal behaviors, such as metallicity, the importance of high-spin configurations, tendency towards orbital differentiation, and the absence of magnetism in regimes which are ordered according to static mean-field theories. Our results are in good agreement with the existing spectroscopic studies and make an essential step towards an understanding of the electronic structures of $Nd_{1-x}Sr_xNiO_2$.

DOI: 10.1103/PhysRevB.102.161118

Introduction. Understanding high-temperature (high-T_c) superconductors is an outstanding question in the area of quantum materials and presents major unsolved questions. With the discovery of new materials, multiple questions arise: what are the origins of high-T_c superconductivity and what are the competing orders? An understanding of these questions requires a proper description of the low-energy electronic structure and the correlations presented in the normal state. The recent discovery of superconductivity in the infinite-layer nickelates, $Nd_{1-x}Sr_xNiO_2$, by Hwang's group [1] raises these questions in a novel context [2].

We have by now, at least four broad classes of unconventional superconducting materials, which have well-established phenomenologies: (1) quasi-one-dimensional organics [3]; (2) materials proximate to a Mott-Hubbard or a charge-transfer insulator [4] such as quasi-two-dimensional organic salts [5] and copper oxide based materials [6–8] which can be described, at low energies, in terms of an effective single band system; (3) intermetallics including rare-earth or actinide heavy-fermion systems [9]; and (4) the more recently discovered iron pnictides and chalcogenides [10,11]. Numerous efforts have been made to synthesize $3d^9$ nickelate materials that can serve as analogs of the doped copper oxide superconductors, such as $La_4Ni_3O_8$ [12,13].

Early on, $LaNiO_2$ was suggested theoretically to be a cuprate analog by Ansisimov *et al.* [14]. However, Lee and Pickett [15] showed that the electronic structure of $LaNiO_2$ differs significantly from the cuprates, as rare-earth 5d bands were shown to cross the Fermi level as well. Other differences include smaller c axis and a more three-dimensional nature, smaller crystal field splitting, and much smaller hybridization strength between the Ni-3d and O-2p states [16]. Alternatively, analogies with heavy-fermion materials have also been proposed [17]. Despite extensive investigations by experiments [18–26], density functional theory (DFT) [16,27–38], GW [34,39], DFT plus dynamical mean-field theory (DFT + DMFT) [40–42] methods [43–51], and theoretical models [17,38,52–56], the nature of the electronic correlations in $Nd_{1-x}Sr_xNiO_2$ still remains an open question. This is partially due to the absence of quantitative comparisons between experiments and theoretical predictions.

In this work, we carry out various electronic structure calculations and analyze the available data for the infinite-layer nickelates at the two ends of hole doping ($LaNiO_2$ and $SrNiO_2$, respectively) as well as the intermediate doping regime. Starting with $SrNiO_2$ that is found to be a typical multiorbital Hund's metal, as a reference, we find that the total Ni-3d occupancy is almost unchanged from $SrNiO_2$ to $LaNiO_2$, and hence $La_{1-x}Sr_xNiO_2$ is naturally and conclusively found to be a multiorbital electronic system with characteristic Hund's metal behaviors.

Methods. We study $LaNiO_2$ instead of $NdNiO_2$ to avoid the issue of Nd-4f orbitals [16,38,45]. A previous study [38] has shown that $LaNiO_2$ and $NdNiO_2$ in fact give essentially the same band structure except for the f bands. Although an early study [57] showed that $SrNiO_2$ does not crystallize in the $LaNiO_2$ structure, in this work, for the purpose of comparison, we assume the same crystal structures ($P4/mmm$; see Fig. S1 in [58]) and use the same lattice parameters $a = b = 3.966$ Å and $c = 3.376$ Å [16,59] for both materials. By doing this, we leave the Sr concentration, x, as the only variable in our comparison, such that we can clearly identify the doping effects of Sr on the electronic structure. We perform fully charge self-consistent DFT + DMFT calculations using the code EDMFTF, developed by Haule *et al.* [60] based on the WIEN2K package [61]. We choose a wide hybridization energy window from

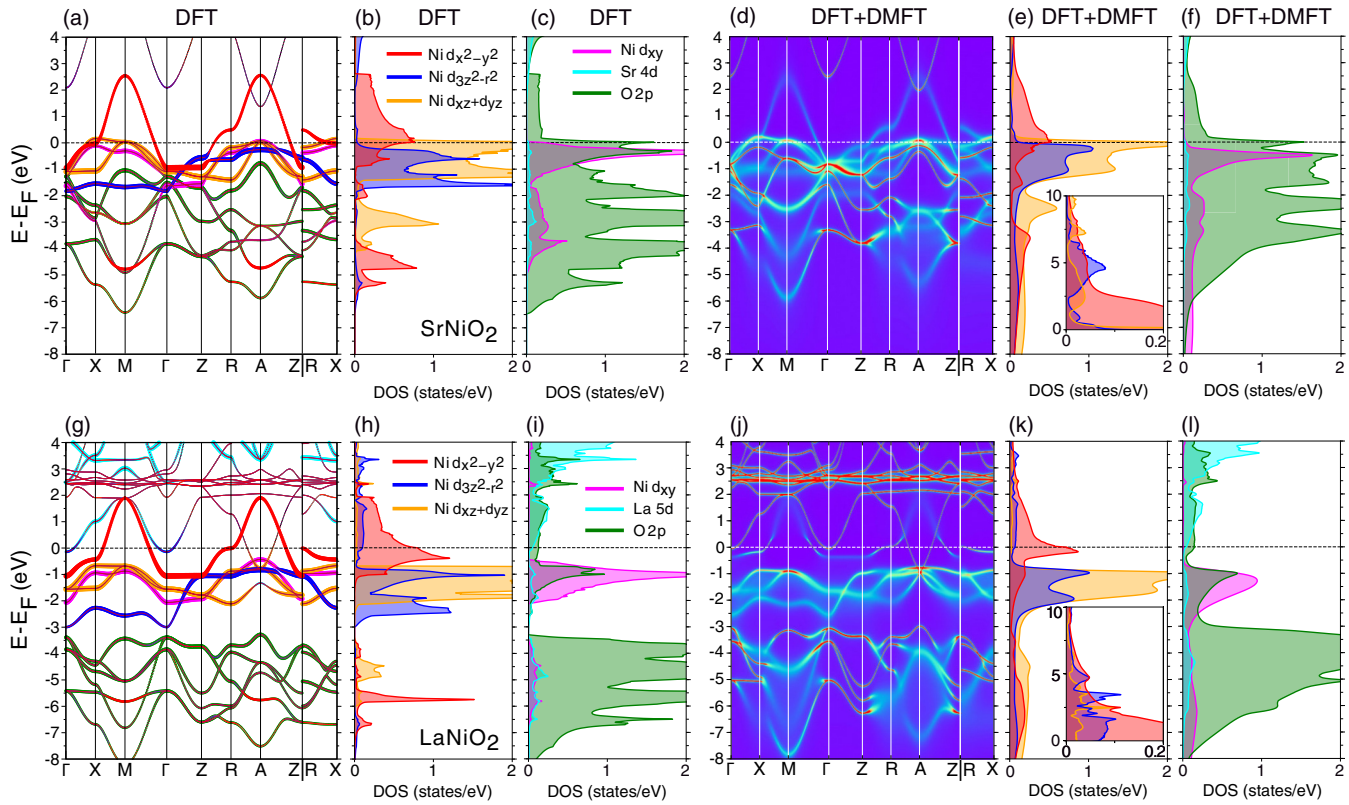

FIG. 1. DFT and DFT + DMFT band structures/k-resolved spectrum functions and density of states. Upper (lower) panels for $SrNiO_2$ ($LaNiO_2$). (a),(g) DFT band structures and (b),(c),(h),(i) DFT density of states. (d),(j) DFT + DMFT k-resolved spectrum functions and (e),(f),(k),(l) DFT + DMFT density of states. The insets in (e) and (k) are the enlarged density of states above the Fermi level from 0 to 10 eV.

−10 to 10 eV with respect to the Fermi level. All five Ni-3d orbitals are considered as correlated ones and a local Coulomb interaction Hamiltonian with rotationally invariant form is applied. We choose $U = 5$ eV and Hund's coupling $J_H = 1$ eV, which are reasonable values for this system [38,47,58]. The local Anderson impurity model is solved by the continuous time quantum Monte Carlo (CTQMC) solver [60,62]. We use an "exact" double counting (DC) scheme invented by Haule [63], which shows better agreement between theory and experiment than the "nominal" or "fully localized limit" schemes [63] and works very well for nickelates [64]. The DFT + DMFT results shown in this work are performed at the temperature $T = 100$ K. The self-energy on real frequency $\Sigma(\omega)$ is obtained by the analytical continuation method of maximum entropy [60]. The local effective mass enhancement due to electronic correlations is defined as $m^*/m^{\mathrm{DFT}} = 1/Z$, where Z is quasiparticle weight. The Sr-doping effects are simulated by the virtual crystal approximation in the intermediate doping regime ($x \leqslant 0.5$).

We also perform spin-polarized calculations to check the energetics of long-range magnetic orders on the static mean-field level using the GGA + U method implemented in the VASP package [65]. A $\sqrt{2} \times \sqrt{2} \times 2$ supercell is used [16,45]. Four magnetic configurations are considered: (i) ferromagnetic (FM), (ii) FM in plane and antiferromagnetic out of plane (AFM-A), (iii) AFM in plane and FM out of plane (AFM-C), and (iv) AFM in plane and AFM out of plane (AFM-G). Computational details are presented in the Supplemental Material [58].

Multiorbital nature and Hund's metal behavior. We start with describing the electronic structure and correlation effects of the material at the extremely hole-doping end, $SrNiO_2$, as a reference system. Figures 1(a)–1(c) show its DFT band structure and density of states (DOS) that are similar to those of $CaCuO_2$ [16], but with one electron removed (nominal $3d^8$). It shows an obvious multiorbital electronic structure with the Fermi level crossing both the e_g and t_{2g} orbitals. The hybridization between Ni-3d and Sr-4d states is very weak, while the Ni-3d states strongly hybridize with the O-2p states with a sharp peak in the O-2p DOS at the Fermi level [see Fig. 1(c)], such that the charge-transfer energy, Δ_{dp}, between the Ni-3d and O-2p states is small (2–3 eV) [16] compared to Hubbard U, indicating a possible charge-transfer Mott-insulator scenario like that in NiO [66,67] if a large Mott gap could be opened. However, our DFT + DMFT calculations show that it is a moderately correlated multiorbital metal.

Table I shows the local occupancy numbers, n_d, and the mass enhancement, m^*/m^{DFT}, of Ni-3d orbitals, and Table II shows the probability of the Ni-3d local multiplets, obtained from the DFT + DMFT calculations. The strong 3d-2p hybridization leads to a much larger Ni-3d total occupancy (8.479) than the nominal value. Except for the d_{xy} orbital, all the other 3d orbitals are partially occupied and moderately renormalized due to the comparable strengths of Hund's coupling and crystal field splitting. There are 1.057 (0.943), 1.755 (0.245), and 1.845 (0.155) electrons (holes) residing on the $d_{x^2-y^2}$, $d_{3z^2-r^2}$, and $d_{xz/yz}$ orbitals, respectively. These

TABLE I. The local occupancy numbers, n_d, and the mass enhancement, $m^*/m^{\rm DFT} = 1/Z$, of Ni-3d orbitals from DFT+DMFT calculations.

		$d_{x^2-y^2}$	$d_{3z^2-r^2}$	d_{xz}	d_{yz}	d_{xy}	Total
n_d	$SrNiO_2$	1.057	1.755	1.845	1.845	1.977	8.479
	$LaNiO_2$	1.219	1.637	1.891	1.891	1.955	8.593
$m^*/m^{\rm DFT}$	$SrNiO_2$	1.89	1.56	1.58	1.58	1.32	
	$LaNiO_2$	2.81	1.25	1.21	1.21	1.27	

holes are highlighted by the DOS above the Fermi level in the inset of Fig. 1(e). In the presence of large Hund's coupling, they form substantial spin-triplet states ($S = 1$) with a weight of 25.4%, while a smaller weight (17.1%) of spin-singlet states in the $N = 8$ sector (see Table II). The Hund's effect is also seen in the DFT + DMFT spectrum functions [see Figs. 1(d) and 1(e)], where the $d_{3z^2-r^2}$ band is pushed closer to the Fermi level compared to the DFT results [Fig. 1(a)]. We find strong charge fluctuations with 7.7%, 43.7%, and 5.6% multiplets in the $N = 7$, 9, and 10 sectors, respectively. The electronic correlation strengths exhibit orbital differentiation, with a larger mass enhancement of 1.89 for the $d_{x^2-y^2}$ orbital and a smaller one of about 1.6 for the $d_{3z^2-r^2}$ and $d_{xz/yz}$ orbitals. Figures 1(d)–1(f) show that all the 3d orbitals except d_{xy} contribute to the DFT + DMFT Fermi surfaces (see Fig. S3 in [58]) and that Δ_{dp} is further reduced by the electronic correlation effects.

Thus, $SrNiO_2$ has many things in common with a correlated multiorbital metal and manifests Hund's metal behavior [68–74], analogous to iron pnictides and chalcogenides, since it (i) is away from half-filling; (ii) has significant enhancement of electronic correlation and mass; (iii) shows important roles of Hund's coupling and high-spin configurations; and (iv) shows orbital differentiation behavior.

We now go to the other end of the undoped $LaNiO_2$ and examine the evolution of band structures from $SrNiO_2$ to $LaNiO_2$ by comparing the DFT band structure and DOS in Figs. 1(g)–1(i) to those in Figs. 1(a)–1(c). The main changes are (i) the Fermi level moves up; (ii) the Ni $d_{x^2-y^2}$ band is pushed away slightly from the other 3d bands; (iii) the La-5d bands start to strongly hybridize with the Ni-3d bands and contribute to the Fermi surfaces [see Γ and A points in Fig. 1(g)]; and (iv) the O-2p bands are pushed down a lot to be nearly isolated from the Ni-3d bands and the 3d-2p hybridization becomes much weaker such that Δ_{dp} is significantly increased. This, in turn, indicates that the 3d-2p hybridization is increasing as increasing the Sr doping level, x, which is clearly evidenced by an emergent pre-

TABLE II. The weights of the Ni-3d local multiplets sampled by CTQMC solver.

Occupancy N	7	8	8	9	10
Total spin S	All	1	0	1/2	0
$SrNiO_2$, DMFT	7.7%	25.4%	17.1%	43.7%	5.6%
$LaNiO_2$, DMFT	6.2%	25.9%	10.3%	49.0%	8.1%
$LaNiO_2$, Ref. [18]	6.0%	24.0%	14.0%	56.0%	

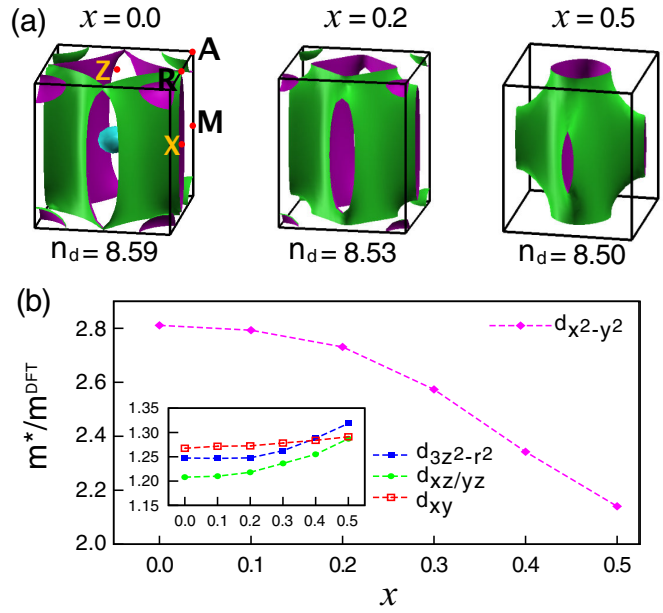

FIG. 2. (a) Evolution of the DFT + DMFT Fermi surfaces and (b) mass enhancement of Ni-3d orbitals vs doping level x in $La_{1-x}Sr_xNiO_2$.

peak in the electron energy loss spectroscopy (EELS) on the oxygen-K edge when $x \geqslant 0.2$ [23]. Here, we also reveal a similar multiorbital nature of $SrNiO_2$, even in the undoped $LaNiO_2$.

Increasing hybridization with unoccupied La-5d states and decreasing hybridization with occupied O-2p states in $LaNiO_2$ will lead to electron transfer from the Ni-3d states to La-5d and O-2p states, so the DFT + DMFT calculations give a Ni-3d total occupancy of 8.593 that is greater than $SrNiO_2$ (8.479) by only 0.11 electrons, even though one more electron is residing in $LaNiO_2$. The DFT calculations also give closer Ni-3d total occupancy for the two materials, with 8.325 and 8.222 electrons for $LaNiO_2$ and $SrNiO_2$, respectively. This suggests that the Ni-3d total occupancy is almost pinned from the undoped end to the extremely doped end, which has also been confirmed by our doping calculations. The overall change of the Ni-3d total occupancy is only 0.09 in the doping range from $x = 0$ to $x = 0.5$ [see Fig. 2(a)]. Comparing to $SrNiO_2$, the occupancy numbers among 3d orbitals in $LaNiO_2$ are slightly redistributed, with 0.162 (0.046) more electrons residing on $d_{x^2-y^2}$ ($d_{xz/yz}$) orbitals and 0.118 less electrons residing on the $d_{3z^2-r^2}$ orbital, so still with substantial holes residing on these orbitals, as highlighted in the inset of Fig. 1(k). As a result, the probability distribution of the Ni-3d multiplets shown in Table II is not too different between $LaNiO_2$ and $SrNiO_2$, so $LaNiO_2$ also shows multiorbital nature and strong metallicity. The calculated weight of the spin-triplet configurations is 25.9% for $LaNiO_2$, which is very close to the value 24% given by the multiplet calculation used to simulate the x-ray absorption and resonant inelastic x-ray scattering (RIXS) spectra of $LaNiO_2$ in [18]. Their simulations show that substantial $3d^8$ spin-triplet configurations are responsible for the resonant prepeak, A', of RIXS. The critical roles of spin-triplet configurations have also been pointed out in [53].

Different from [43], we obtain a small percentage of the $3d^{10}$ configuration (8.1%) that rules out the possibility of the charge-transfer Mott-insulator scenario in $LaNiO_2$. The percentages of other multiplets obtained here are also very close to the values given by [18], which validates our DFT + DMFT calculations.

Going from $SrNiO_2$ to $LaNiO_2$, the orbital differentiation is significantly enhanced, with stronger mass enhancement of 2.81 for the $d_{x^2-y^2}$ orbital and weaker mass enhancement of about 1.2–1.3 for the other $3d$ orbitals in $LaNiO_2$. Figure 2(b) shows that a tendency of increasing correlation in the $d_{x^2-y^2}$ orbital and decreasing correlation in other $3d$ orbitals, as decreasing hole-doping level x, has been captured by our doping calculations. As shown in the DFT + sicDMFT calculations by Lechermann [50,51], a large enough Hubbard U ($\geqslant 10\,\mathrm{eV}$) may open a Mott gap in the $d_{x^2-y^2}$ orbital. Our results strongly support their claim that the multiorbital nature rules the normal state of $NdNiO_2$ [50,51], but with strong metallicity in the $d_{x^2-y^2}$ orbital found in our work. Figure 2(a) shows the evolution of the DFT + DMFT Fermi surface as increasing hole doping. We find Lifshitz transitions of the Fermi surface from $x = 0$ to $x = 0.5$ and two sheets of Fermi surfaces around the optimal doping level, $x \approx 0.2$. Our results of occupancy numbers and mass enhancement of Ni $d_{x^2-y^2}$ and $d_{3z^2-r^2}$ orbitals as well as the evolution of Fermi surfaces as increasing hole doping are consistent with the previous DFT + DMFT study with $U = 6\,\mathrm{eV}$, $J_H = 0.95\,\mathrm{eV}$, and a fully localized DC scheme [47].

Magnetism. One of the main arguments to question the cupratelike superconducting nature in $Nd_{1-x}Sr_xNiO_2$ is that the superexchange coupling J_{ex} is too small due to the very large Δ_{dp} [53]. Here, like $CaCuO_2$ [16,43], Δ_{dp} is significantly decreased in $SrNiO_2$, which may stabilize long-range AFM orders or induce stronger AFM fluctuations through an enhanced J_{ex}. We check this by comparing the ground state energy of possible magnetic configurations in $SrNiO_2$ to that in $LaNiO_2$ on the static mean-field (GGA + U) level. Figures 3(a) and 3(b) show the energy difference per one Ni site between the magnetic and nonmagnetic (NM) states, $\delta E = E_{\mathrm{M}} - E_{\mathrm{NM}}$, as functions of Hubbard U. For $SrNiO_2$, the lowest energy state is FM and AFM-A when $U \leqslant 3\,\mathrm{eV}$ and AFM-G when $U > 3\,\mathrm{eV}$. For $LaNiO_2$, AFM-G is the lowest energy state, even at the GGA level ($U = 0$) [45]. FM, AFM-A, and AFM-C are also lower in energy than the nonmagnetic state when $U > 0$. δE of $LaNiO_2$ becomes much larger than that of $SrNiO_2$ when $U > 0$, which suggests that it is much harder for $SrNiO_2$ to stabilize magnetic orders than $LaNiO_2$ even though $SrNiO_2$ has a smaller Δ_{dp}, hence the physics of superexchange is not operational in these materials, while they are essential for the cuprates.

Although the static mean-field calculations can give stable long-range magnetic orders with large ordered magnetic moments [see Figs. 3(c) and 3(d)] in both $LaNiO_2$ and $SrNiO_2$, in reality, no signature of such orders has been observed in $LaNiO_2$ or $NdNiO_2$ down to the very low temperature range the available experiments have approached so far [75,76]. This situation is similar to that in iron-based superconductors, where the static mean-field calculations usually predict stable magnetic orders with large ordered moments while the moments are found to be significantly suppressed in experiments, as discussed widely in literature [71,77–83].

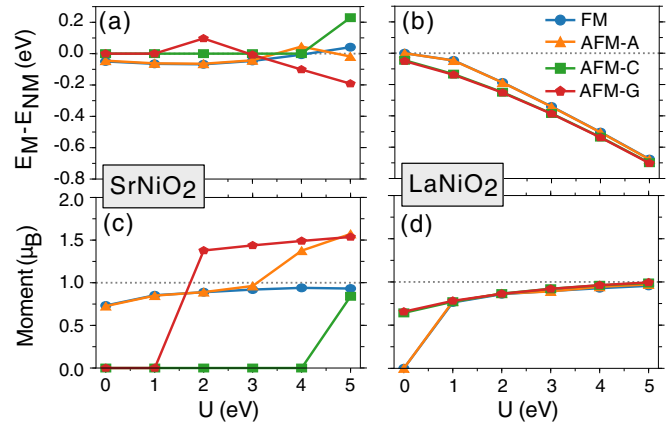

FIG. 3. (a),(b) The total energy difference (per the unit cell containing one Ni site) between the magnetic states and the nonmagnetic state, $E_{\mathrm{M}} - E_{\mathrm{NM}}$, vs Hubbard U from GGA + U calculations. (c),(d) The ordered magnetic moments per one Ni site vs U. (a),(c) for $SrNiO_2$ and (b),(d) for $LaNiO_2$.

Conclusion and discussion. To summarize, we have provided a perspective to describe the normal state electronic structure of $La_{1-x}Sr_xNiO_2$ starting using $SrNiO_2$ as a reference. $SrNiO_2$ is found to be a moderately correlated multiorbital Hund-like metal. Going from $SrNiO_2$ to $LaNiO_2$, the Ni-$3d$ total occupancy is insensitive to decreasing hole doping as the changes in carrier density are compensated by decreased hybridization with the occupied O-$2p$ states and increased hybridization with the unoccupied La-$5d$ states. Thus, as in $SrNiO_2$, the same amount of high-spin configurations, same order of charge fluctuation, and similar multiorbital nature but with enhanced orbital differentiation, are found in $LaNiO_2$. From this perspective, $La_{1-x}Sr_xNiO_2$ is naturally and conclusively found to be a multiorbital electronic system with characteristic Hund's metal behaviors. Therefore, our study excludes the cupratelike scenario for this new Ni based superconductor and suggests that $Nd_{1-x}Sr_xNiO_2$ is a new unconventional superconductor that shares many similarities with iron-based superconductors [10,11,54,84–86], such as their metallicity, the importance of Hund's coupling and high-spin configurations, tendency towards orbital differentiation with the $d_{x^2-y^2}$ orbital as the most correlated orbital, and the absence of magnetism in regimes which are ordered according to static mean-field theories. Despite many similarities, there are critical differences such as magnetic orders, Fermi surfaces topology, and low-energy subspace (e_g rather than t_{2g} orbitals in $Nd_{1-x}Sr_xNiO_2$) between the iron-based superconductors and $Nd_{1-x}Sr_xNiO_2$, which make the latter a unique unconventional superconductor.

Our calculated Ni-$3d$ multiplet weights and trend of increasing $3d$-$2p$ hybridization upon Sr doping show quantitatively and qualitatively good agreement with the RIXS data [18] and the EELS observations [23], respectively. Most interestingly, the ratio between the largest superconducting gap $2\Delta_{\mathrm{max}}$ and T_c (determined as the midpoint of the superconducting transition in resistivity) is evaluated to be about 7 from

the most recent experimental data of $Nd_{1-x}Sr_xNiO_2$ [87], which is very close to the value for the iron-based superconductors [86,88] and hence supports our findings. Considering the fact that only limited experiments are available for this system, in particular the band structure measurement is still missing, our calculations that are in good agreement with the existing experiments make an essential step towards an understanding of the electronic structure of $Nd_{1-x}Sr_xNiO_2$ and pave the way to understand its superconducting pairing mechanism.

Finally, we notice that as we place $Nd_{1-x}Sr_xNiO_2$ far from a Mott transition, the insulating behavior observed at low doping and temperatures has to be attributed to the impurity-induced Anderson localization, which should get weaker as sample quality improves.

Note added. Recently, we learned about the related parameter-free *GW* + EDMFT work [89] that also finds multiorbital nature and the pinning of the Ni-3*d* total occupancy in the small doping regime of $Nd_{1-x}Sr_xNiO_2$, which validates our simple DFT + DMFT calculations.

Acknowledgments. We thank Kristjan Haule and Sangkook Choi for very helpful discussions. Y.W., C.K., and G.K. were supported by the US Department of Energy, Office of Science, Basic Energy Sciences as a part of the Computational Materials Science Program through the Center for Computational Design of Functional Strongly Correlated Materials and Theoretical Spectroscopy. H.M. was sponsored by the Laboratory Directed Research and Development Program of ORNL, managed by UT-Battelle, LLC, for the US Department of Energy.

[1] D. Li, K. Lee, B. Y. Wang, M. Osada, S. Crossley, H. R. Lee, Y. Cui, Y. Hikita, and H. Y. Hwang, Superconductivity in an infinite-layer nickelate, Nature (London) **572**, 624 (2019).

[2] M. R. Norman, Entering the nickel age of superconductivity, Physics **13**, 85 (2020).

[3] D. Jérome, The physics of organic superconductors, Science **252**, 1509 (1991).

[4] J. Zaanen, G. A. Sawatzky, and J. W. Allen, Band Gaps and Electronic Structure of Transition-Metal Compounds, Phys. Rev. Lett. **55**, 418 (1985).

[5] B. J. Powell and R. H. McKenzie, Strong electronic correlations in superconducting organic charge transfer salts, J. Phys.: Condens. Matter **18**, R827 (2006).

[6] J. G. Bednorz and K. A. Müller, Possible high-T_c superconductivity in the Ba-La-Cu-O system, Z. Phys. B **64**, 189 (1986).

[7] P. A. Lee, N. Nagaosa, and X.-G. Wen, Doping a Mott insulator: Physics of high-temperature superconductivity, Rev. Mod. Phys. **78**, 17 (2006).

[8] E. Dagotto, Correlated electrons in high-temperature superconductors, Rev. Mod. Phys. **66**, 763 (1994).

[9] G. R. Stewart, Heavy-fermion systems, Rev. Mod. Phys. **56**, 755 (1984).

[10] Y. Kamihara, T. Watanabe, M. Hirano, and H. Hosono, Iron-based layered superconductor $La[O_{1-x}F_x]FeAs$ ($x = 0.05$-0.12) with $T_c = 26$ K, J. Am. Chem. Soc. **130**, 3296 (2008).

[11] G. R. Stewart, Superconductivity in iron compounds, Rev. Mod. Phys. **83**, 1589 (2011).

[12] V. V. Poltavets, K. A. Lokshin, A. H. Nevidomskyy, M. Croft, T. A. Tyson, J. Hadermann, G. Van Tendeloo, T. Egami, G. Kotliar, N. ApRoberts-Warren, A. P. Dioguardi, N. J. Curro, and M. Greenblatt, Bulk Magnetic Order in a Two-Dimensional $Ni^{1+}/Ni^{2+}(d^9/d^8)$ Nickelate, Isoelectronic with Superconducting Cuprates, Phys. Rev. Lett. **104**, 206403 (2010).

[13] J. Zhang, D. M. Pajerowski, A. S. Botana, H. Zheng, L. Harriger, J. Rodriguez-Rivera, J. P. C. Ruff, N. J. Schreiber, B. Wang, Y.-S. Chen, W. C. Chen, M. R. Norman, S. Rosenkranz, J. F. Mitchell, and D. Phelan, Spin Stripe Order in a Square Planar Trilayer Nickelate, Phys. Rev. Lett. **122**, 247201 (2019).

[14] V. I. Anisimov, D. Bukhvalov, and T. M. Rice, Electronic structure of possible nickelate analogs to the cuprates, Phys. Rev. B **59**, 7901 (1999).

[15] K.-W. Lee and W. E. Pickett, Infinite-layer $LaNiO_2$: Ni^{1+} is not Cu^{2+}, Phys. Rev. B **70**, 165109 (2004).

[16] A. S. Botana and M. R. Norman, Similarities and Differences between $LaNiO_2$ and $CaCuO_2$ and Implications for Superconductivity, Phys. Rev. X **10**, 011024 (2020).

[17] G.-M. Zhang, Y.-feng Yang, and F.-C. Zhang, Self-doped Mott insulator for parent compounds of nickelate superconductors, Phys. Rev. B **101**, 020501(R) (2020).

[18] M. Hepting, D. Li, C. J. Jia, H. Lu, E. Paris, Y. Tseng, X. Feng, M. Osada, E. Been, Y. Hikita *et al.*, Electronic structure of the parent compound of superconducting infinite-layer nickelates, Nat. Mater. **19**, 381 (2020).

[19] Y. Fu, L. Wang, H. Cheng, S. Pei, X. Zhou, J. Chen, S. Wang, R. Zhao, W. Jiang, C. Liu, M. Huang, XinWei Wang, Y. Zhao, D. Yu, F. Ye, S. Wang, and J.-W. Mei, Core-level x-ray photoemission and Raman spectroscopy studies on electronic structures in Mott-Hubbard type nickelate oxide $NdNiO_2$, arXiv:1911.03177.

[20] S. Zeng, C. S. Tang, X. Yin, C. Li, Z. Huang, J. Hu, W. Liu, G. J. Omar, H. Jani, Z. S. Lim, K. Han, D. Wan, P. Yang, A. T. S. Wee, and A. Ariando, Phase Diagram and Superconducting Dome of Infinite-Layer $Nd_{1-x}Sr_xNiO_2$ Thin Films, Phys. Rev. Lett. **125**, 147003 (2020).

[21] D. Li, B. Y. Wang, K. Lee, S. P. Harvey, M. Osada, B. H. Goodge, L. F. Kourkoutis, and H. Y. Hwang, Superconducting Dome in $Nd_{1-x}Sr_xNiO_2$ Infinite Layer Films, Phys. Rev. Lett. **125**, 027001 (2020).

[22] M. Osada, B. Y. Wang, B. H. Goodge, K. Lee, H. Yoon, K. Sakuma, D. Li, M. Miura, L. F. Kourkoutis, and H. Y. Hwang, A superconducting praseodymium nickelate with infinite layer structure, Nano Lett. **20**, 5735 (2020).

[23] B. H. Goodge, D. Li, M. Osada, B. Y. Wang, K. Lee, G. A. Sawatzky, H. Y. Hwang, and L. F. Kourkoutis, Doping evolution of the Mott-Hubbard landscape in infinite-layer nickelates, arXiv:2005.02847.

[24] K. Lee, B. H. Goodge, D. Li, M. Osada, B. Y. Wang, Y. Cui, L. F. Kourkoutis, and H. Y. Hwang, Aspects of the synthesis of thin film superconducting infinite-layer nickelates, APL Mater. **8**, 041107 (2020).

[25] Q. Li, C. He, J. Si, X. Zhu, Y. Zhang, and H.-H. Wen, Absence of superconductivity in bulk $Nd_{1-x}Sr_xNiO_2$, Commun. Mater. **1**, 16 (2020).

[26] B.-X. Wang, H. Zheng, E. Krivyakina, O. Chmaissem, P. P. Lopes, J. W. Lynn, L. C. Gallington, Y. Ren, S. Rosenkranz, J. F. Mitchell, and D. Phelan, Synthesis and characterization of bulk $Nd_{1-x}Sr_xNiO_2$ and $Nd_{1-x}Sr_xNiO_3$, Phys. Rev. Mater. **4**, 084409 (2020).

[27] P. Jiang, L. Si, Z. Liao, and Z. Zhong, Electronic structure of rare-earth infinite-layer $RNiO_2$(R=La,Nd), Phys. Rev. B **100**, 201106(R) (2019).

[28] J. Gao, S. Peng, Z. Wang, C. Fang, and H. Weng, Electronic structures and topological properties in nickelates $Ln_{n+1}Ni_nO_{2n+2}$, National Sci. Rev. (2020), doi:10.1093/nsr/nwaa218.

[29] Y. Nomura, M. Hirayama, T. Tadano, Y. Yoshimoto, K. Nakamura, and R. Arita, Formation of a two-dimensional single-component correlated electron system and band engineering in the nickelate superconductor $NdNiO_2$, Phys. Rev. B **100**, 205138 (2019).

[30] Z. Liu, Z. Ren, W. Zhu, Z. Wang, and J. Yang, Electronic and magnetic structure of infinite-layer $NdNiO_2$: Trace of antiferromagnetic metal, npj Quantum Mater. **5**, 31 (2020).

[31] X. Wu, D. Di Sante, T. Schwemmer, W. Hanke, H. Y. Hwang, S. Raghu, and R. Thomale, Robust $d_{x^2-y^2}$-wave superconductivity of infinite-layer nickelates, Phys. Rev. B **101**, 060504(R) (2020).

[32] M.-Y. Choi, K.-W. Lee, and W. E. Pickett, Role of 4f states in infinite-layer $NdNiO_2$, Phys. Rev. B **101**, 020503(R) (2020).

[33] M.-Y. Choi, W. E. Pickett, and K. W. Lee, Quantum-fluctuation-frustrated flat band instabilities in $NdNiO_2$, Phys. Rev. Res. **2**, 033445 (2020).

[34] M. Hirayama, T. Tadano, Y. Nomura, and R. Arita, Materials design of dynamically stable d^9 layered nickelates, Phys. Rev. B **101**, 075107 (2020).

[35] E. Been, W.-S. Lee, H. Y. Hwang, Y. Cui, J. Zaanen, T. Devereaux, B. Moritz, and C. Jia, Theory of rare-earth infinite layer nickelates, arXiv:2002.12300.

[36] B. Geisler and R. Pentcheva, Fundamental difference in the electronic reconstruction of infinite-layer versus perovskite neodymium nickelate films on $SrTiO_3$(001), Phys. Rev. B **102**, 020502 (2020).

[37] Z.-J. Lang, R. Jiang, and W. Ku, Where do the doped hole carriers reside in the new superconducting nickelates? arXiv:2005.00022.

[38] H. Sakakibara, H. Usui, K. Suzuki, T. Kotani, H. Aoki, and K. Kuroki, Model Construction and a Possibility of Cupratelike Pairing in a New d^9 Nickelate Superconductor (Nd,Sr)NiO_2, Phys. Rev. Lett. **125**, 077003 (2020).

[39] V. Olevano, F. Bernardini, X. Blase, and A. Cano, *Ab initio* many-body *GW* correlations in the electronic structure of $LaNiO_2$, Phys. Rev. B **101**, 161102(R) (2020).

[40] A. Georges, G. Kotliar, W. Krauth, and M. J. Rozenberg, Dynamical mean-field theory of strongly correlated fermion systems and the limit of infinite dimensions, Rev. Mod. Phys. **68**, 13 (1996).

[41] G. Kotliar, S. Y. Savrasov, K. Haule, V. S. Oudovenko, O. Parcollet, and C. A. Marianetti, Electronic structure calculations with dynamical mean-field theory, Rev. Mod. Phys. **78**, 865 (2006).

[42] A. I. Lichtenstein, M. I. Katsnelson, and G. Kotliar, Finite-Temperature Magnetism of Transition Metals: An *ab initio* Dynamical Mean-Field Theory, Phys. Rev. Lett. **87**, 067205 (2001).

[43] J. Karp, A. S. Botana, M. R. Norman, H. Park, M. Zingl, and A. Millis, Many-Body Electronic Structure of $NdNiO_2$ and $CaCuO_2$, Phys. Rev. X **10**, 021061 (2020).

[44] L. Si, W. Xiao, J. Kaufmann, J. M. Tomczak, Y. Lu, Z. Zhong, and K. Held, Topotactic Hydrogen in Nickelate Superconductors and Akin Infinite-Layer Oxides ABO_2, Phys. Rev. Lett. **124**, 166402 (2020).

[45] S. Ryee, H. Yoon, T. J. Kim, M. Y. Jeong, and M. J. Han, Induced magnetic two-dimensionality by hole doping in the superconducting infinite-layer nickelate $Nd_{1-x}Sr_xNiO_2$, Phys. Rev. B **101**, 064513 (2020).

[46] Y. Gu, S. Zhu, X. Wang, J. Hu, and H. Chen, A substantial hybridization between correlated Ni-d orbital and itinerant electrons in infinite-layer nickelates, Commun. Phys. **3**, 84 (2020).

[47] I. Leonov, S. L. Skornyakov, and S. Y. Savrasov, Lifshitz transition and frustration of magnetic moments in infinite-layer $NdNiO_2$ upon hole doping, Phys. Rev. B **101**, 241108(R) (2020).

[48] I. Leonov and S. Y. Savrasov, Effect of epitaxial strain on the electronic structure and magnetic correlations in infinite-layer (Nd,Sr)NiO_2, arXiv:2006.05295.

[49] M. Kitatani, L. Si, O. Janson, R. Arita, Z. Zhong, and K. Held, Nickelate superconductors—A renaissance of the one-band Hubbard model, npj Quantum Mater. **5**, 59 (2020).

[50] F. Lechermann, Late transition metal oxides with infinite-layer structure: Nickelates versus cuprates, Phys. Rev. B **101**, 081110(R) (2020).

[51] F. Lechermann, Multiorbital Processes Rule the $Nd_{1-x}Sr_xNiO_2$ Normal State, Phys. Rev. X **10**, 041002 (2020).

[52] L.-H. Hu and C. Wu, Two-band model for magnetism and superconductivity in nickelates, Phys. Rev. Res. **1**, 032046 (2019).

[53] M. Jiang, M. Berciu, and G. A. Sawatzky, Critical Nature of the Ni Spin State in Doped $NdNiO_2$, Phys. Rev. Lett. **124**, 207004 (2020).

[54] P. Werner and S. Hoshino, Nickelate superconductors: Multiorbital nature and spin freezing, Phys. Rev. B **101**, 041104(R) (2020).

[55] H. Zhang, L. Jin, S. Wang, B. Xi, Xingqiang Shi, F. Ye, and J.-W. Mei, Effective Hamiltonian for nickelate oxides $Nd_{1-x}Sr_xNiO_2$, Phys. Rev. Res. **2**, 013214 (2020).

[56] Y.-H. Zhang and A. Vishwanath, Type-II t-j model in superconducting nickelate $Nd_{1-x}Sr_xNiO_2$, Phys. Rev. Res. **2**, 023112 (2020).

[57] H. Pausch and Hk. Müller-Buschbaum, Präparation von $SrNiO_2$-einkristallen mit eben koordiniertem nickel, Z. Anorg. Allg. Chem. **426**, 184 (1976).

[58] See Supplemental Material at http://link.aps.org/supplemental/10.1103/PhysRevB.102.161118 for the computational details, the choosing of U and J_H, the Fermi surfaces of $LaNiO_2$ and $SRNIO_2$, and the justification of the changes of hybridizations, which includes Refs. [18,38,43,46,47,65,90–97].

[59] P. Levitz, M. Crespin, and L. Gatineau, Structure of $LaNiO_2$ by EXAFS and x-ray diffraction: Local environment of Ni^{+1}, in *EXAFS and Near Edge Structure*, edited by Antonio Bianconi, Lucia Incoccia, and Stanislao Stipcich (Springer, Berlin, Heidelberg, 1983), pp. 219–221.

[60] K. Haule, C.-H. Yee, and K. Kim, Dynamical mean-field theory within the full-potential methods: Electronic structure of

CeIrIn$_5$, CeCoIn$_5$, and CeRhIn$_5$, Phys. Rev. B **81**, 195107 (2010).

[61] P. Blaha, K. Schwarz, F. Tran, R. Laskowski, G. K. H. Madsen, and L. D. Marks, WIEN2k: An APW+lo program for calculating the properties of solids, J. Chem. Phys. **152**, 074101 (2020).

[62] E. Gull, A. J. Millis, A. I. Lichtenstein, A. N. Rubtsov, M. Troyer, and P. Werner, Continuous-time Monte Carlo methods for quantum impurity models, Rev. Mod. Phys. **83**, 349 (2011).

[63] K. Haule, Exact Double Counting in Combining the Dynamical Mean Field Theory and the Density Functional Theory, Phys. Rev. Lett. **115**, 196403 (2015).

[64] K. Haule and G. L. Pascut, Mott transition and magnetism in rare earth nickelates and its fingerprint on the x-ray scattering, Sci. Rep. **7**, 10375 (2017).

[65] G. Kresse and J. Furthmüller, Efficient iterative schemes for *ab initio* total-energy calculations using a plane-wave basis set, Phys. Rev. B **54**, 11169 (1996).

[66] M. Imada, A. Fujimori, and Y. Tokura, Metal-insulator transitions, Rev. Mod. Phys. **70**, 1039 (1998).

[67] T. M. Schuler, D. L. Ederer, S. Itza-Ortiz, G. T. Woods, T. A. Callcott, and J. C. Woicik, Character of the insulating state in NiO: A mixture of charge-transfer and Mott-Hubbard character, Phys. Rev. B **71**, 115113 (2005).

[68] P. Werner, E. Gull, M. Troyer, and A. J. Millis, Spin Freezing Transition and Non-Fermi-Liquid Self-Energy in a Three-Orbital Model, Phys. Rev. Lett. **101**, 166405 (2008).

[69] K. Haule and G. Kotliar, Coherence-incoherence crossover in the normal state of iron oxypnictides and importance of Hund's rule coupling, New J. Phys. **11**, 025021 (2009).

[70] L. de' Medici, J. Mravlje, and A. Georges, Janus-Faced Influence of Hund's Rule Coupling in Strongly Correlated Materials, Phys. Rev. Lett. **107**, 256401 (2011).

[71] Z. P. Yin, K. Haule, and G. Kotliar, Kinetic frustration and the nature of the magnetic and paramagnetic states in iron pnictides and iron chalcogenides, Nat. Mater. **10**, 932 (2011).

[72] A. Georges, L. de' Medici, and J. Mravlje, Strong correlations from Hund's coupling, Annu. Rev. Condens. Matter Phys. **4**, 137 (2013).

[73] L. de' Medici, Hund's metals, explained, in *The Physics of Correlated Insulators, Metals, and Superconductors*, edited by E. Pavarini, E. Koch, R. Scalettar, and R. Martin (Forschungszentrum Jülich GmbH Zentralbibliothek, Verlag, Jülich, 2017), Vol. 7.

[74] K. M. Stadler, G. Kotliar, A. Weichselbaum, and J. von Delft, Hundness versus Mottness in a three-band Hubbard-Hund model: On the origin of strong correlations in Hund metals, Ann. Phys. **405**, 365 (2019).

[75] M. A. Hayward, M. A. Green, M. J. Rosseinsky, and J. Sloan, Sodium hydride as a powerful reducing agent for topotactic oxide deintercalation: Synthesis and characterization of the nickel(I) oxide LaNiO$_2$, J. Am. Chem. Soc. **121**, 8843 (1999).

[76] M. A. Hayward and M. J. Rosseinsky, Synthesis of the infinite layer Ni(I) phase NdNiO$_{2+x}$ by low temperature reduction of NdNiO$_3$ with sodium hydride,Solid State Sci. **5**, 839 (2003).

[77] S. Ishibashi, K. Terakura, and H. Hosono, A possible ground state and its electronic structure of a mother material (LaOFeAs) of new superconductors, J. Phys. Soc. Jpn. **77**, 053709 (2008).

[78] Q. Huang, Y. Qiu, W. Bao, M. A. Green, J. W. Lynn, Y. C. Gasparovic, T. Wu, G. Wu, and X. H. Chen, Neutron-Diffraction Measurements of Magnetic Order and a Structural Transition in the Parent BaFe$_2$As$_2$ Compound of FeAs-Based High-Temperature Superconductors, Phys. Rev. Lett. **101**, 257003 (2008).

[79] K. Ishida, Y. Nakai, and H. Hosono, To what extent iron-pnictide new superconductors have been clarified: A progress report, J. Phys. Soc. Jpn. **78**, 062001 (2009).

[80] N. Qureshi, Y. Drees, J. Werner, S. Wurmehl, C. Hess, R. Klingeler, B. Büchner, M. T. Fernández-Díaz, and M. Braden, Crystal and magnetic structure of the oxypnictide superconductor LaFeAsO$_{1-x}$F$_x$: A neutron-diffraction study, Phys. Rev. B **82**, 184521 (2010).

[81] S. V. Borisenko, V. B. Zabolotnyy, D. V. Evtushinsky, T. K. Kim, I. V. Morozov, A. N. Yaresko, A. A. Kordyuk, G. Behr, A. Vasiliev, R. Follath, and B. Büchner, Superconductivity without Nesting in LiFeAs, Phys. Rev. Lett. **105**, 067002 (2010).

[82] P. Hansmann, R. Arita, A. Toschi, S. Sakai, G. Sangiovanni, and K. Held, Dichotomy between Large Local and Small Ordered Magnetic Moments in Iron-Based Superconductors, Phys. Rev. Lett. **104**, 197002 (2010).

[83] A. Toschi, R. Arita, P. Hansmann, G. Sangiovanni, and K. Held, Quantum dynamical screening of the local magnetic moment in Fe-based superconductors, Phys. Rev. B **86**, 064411 (2012).

[84] Q. Si, R. Yu, and E. Abrahams, High-temperature superconductivity in iron pnictides and chalcogenides, Nat. Rev. Mater. **1**, 16017 (2016).

[85] S. Hoshino and P. Werner, Superconductivity from Emerging Magnetic Moments, Phys. Rev. Lett. **115**, 247001 (2015).

[86] T.-H. Lee, A. Chubukov, H. Miao, and G. Kotliar, Pairing Mechanism in Hund's Metal Superconductors and the Universality of the Superconducting Gap to Critical Temperature Ratio, Phys. Rev. Lett. **121**, 187003 (2018).

[87] Qiangqiang Gu, Y. Li, S. Wan, H. Li, W. Guo, H. Yang, Q. Li, X. Zhu, X. Pan, Y. Nie, and H.-H. Wen, Two superconducting components with different symmetries in Nd$_{1-x}$Sr$_x$NiO$_2$ films, arXiv:2006.13123.

[88] H. Miao, W. H. Brito, Z. P. Yin, R. D. Zhong, G. D. Gu, P. D. Johnson, M. P. M. Dean, S. Choi, G. Kotliar, W. Ku, X. C. Wang, C. Q. Jin, S.-F. Wu, T. Qian, and H. Ding, Universal $2\Delta_{\max}/k_BT_c$ scaling decoupled from the electronic coherence in iron-based superconductors, Phys. Rev. B **98**, 020502(R) (2018).

[89] F. Petocchi, V. Christiansson, F. Nilsson, F. Aryasetiawan, and P. Werner, Normal state of Nd$_{1-x}$Sr$_x$NiO$_2$ from self-consistent GW + EDMFT, arXiv:2006.00394.

[90] K. Momma and F. Izumi, VESTA: A three-dimensional visualization system for electronic and structural analysis, J. Appl. Crystallogr. **41**, 653 (2008).

[91] P. E. Blöchl, Projector augmented-wave method, Phys. Rev. B **50**, 17953 (1994).

[92] G. Kresse and D. Joubert, From ultrasoft pseudopotentials to the projector augmented-wave method, Phys. Rev. B **59**, 1758 (1999).

[93] J. P. Perdew, K. Burke, and M. Ernzerhof, Generalized Gradient Approximation Made Simple, Phys. Rev. Lett. **77**, 3865 (1996).

[94] S. Sugano, Y. Tanabe, and H. Kamimura, *Multiplets of Transition-Metal Ions in Crystals* (Academic, New York, 1970).

[95] F. M. F. de Groot, J. C. Fuggle, B. T. Thole, and G. A. Sawatzky, 2p x-ray absorption of 3d transition-metal compounds: An

atomic multiplet description including the crystal field, Phys. Rev. B **42**, 5459 (1990).

[96] Y. Wang, Z. Wang, Z. Fang, and X. Dai, Interaction-induced quantum anomalous Hall phase in (111) bilayer of $LaCoO_3$, Phys. Rev. B **91**, 125139 (2015).

[97] F. Aryasetiawan, M. Imada, A. Georges, G. Kotliar, S. Biermann, and A. I. Lichtenstein, Frequency-dependent local interactions and low-energy effective models from electronic structure calculations, Phys. Rev. B **70**, 195104 (2004).